ISSN 0016-7932, Geomagnetism and Aeronomy, 2013, Vol. 53, No. 2, pp. 204–215. © Pleiades Publishing, Ltd., 2013.
Original Russian Text © N. Blaunstein, S.A. Pulinets, Y. Cohen, 2013, published in Geomagnetizm i Aeronomiya, 2013, Vol. 53, No. 2, pp. 215–227.

Computation of the Key Parameters of Radio Signals Propagating through a Perturbed Ionosphere in the Land–Satellite Channel

N. Blaunstein[a], S. A. Pulinets[b], and Y. Cohen[a]

[a] *Ben Gurion University of the Negev, Beer-Sheva, Israel*
[b] *Space Research Institute, Russian Academy of Sciences, Moscow, Russia*
e-mail: natanb@cse.bgu.ac.il, pulse@rssi.ru

Received January 19, 2012; in final form, June 13, 2012

Abstract—An analysis of the key parameters of HF/UHF radio signals was carried out for land–satellite radio channels, which determine the effects of fading in a perturbed ionosphere. Using the parameters of the perturbed plasma, the effects of the absorption and phase fluctuations of radio signals are analyzed for a channel with fading. For the evaluation of the effect of scattering of a radio signal by ionospheric inhomogeneities in an approximation of small-scale scintillations, expressions for the root-mean-square (RMS) magnitude of signal intensity and phase scintillations are presented. Scintillation index σ_I^2 that corresponds to variations in a signal under the conditions of multipath propagation with fading is investigated by using experimental data. It is shown that roughly ~10% of inhomogeneities of the electron concentration in the *F* region of the ionosphere, perturbed during a magnetic storm, yield strong quickly fading radio signals in the VHF/UHF range with significant fluctuations (up to 1%) in the intensity of the signal and phase fluctuations (up to hundreds of radians). The calculated magnitudes of the scintillation index are in good agreement with experimentally observed data.

DOI: 10.1134/S0016793213020047

1. INTRODUCTION

The ionosphere is one of the channels (in addition to the terrestrial and atmospheric ones) of global multimode radiowave propagation in the satellite–land system. It is well known that ionospheric inhomogeneities cause strong fluctuations in the amplitude and phase of a signal. An increase in the intensity of inhomogeneities is usually observed during periods of magnetic perturbations, especially in the auroral ionosphere (see (Kintner and Ledivina, 2005; Basu et al., 2001; Ledivina et al., 2002; Erickson et al., 2002; Foster and Burke, 2002; Mishin et al., 2003; Mishin and Burke, 2005; Pfaff et al., 2008; Mishin and Blaunstein, 2008) and references therein). If during magnetic perturbations the auroral boundaries shift equatorward, then, as a rule, it is usually assumed that midlatitude scintillation events occur inside the expanded auroral zone.

A fully expected fact (according to the publications of many researchers dealing with satellite observations of the perturbed ionosphere) is that the described fluctuations are observed not only in the proximity of the polar and auroral zones, but also in the subauroral zone and at midlatitudes (Hardy et al., 1984; Rich and Hairston, 1994; Maynard et al., 1996; Forser and Rich, 1998; Saunders, 1999). The rate of their appearance is of about 15–17% per year with durations from several days to several weeks. It was found that during magnetic storms strong phase and amplitude scintillations (the scintillation index $S_4 \geq 0.5$) of radio signals are observed from satellites, operating at 250 MHz (Basu et al., 2001) and 1.5 GHz (Ledivina et al., 2002) at significant distances far from the polar zone directed to the equator, i.e., in the subauroral and midlatitude ionosphere. Satellite and radar observations in the perturbed auroral ionosphere (Erickson et al., 2002; Foster and Burke, 2002; Mishin et al., 2003; Mishin and Burke, 2005) revealed irregular plasma structures embedded within fast westward streams, called subauroral polarization streams (SAPS's) (Foster and Burke, 2002). In particular, strongly irregular plasma density structures are hidden within SAPS wave-like structures (called SAPSWS's) (Foster and Burke, 2002; Mishin and Burke, 2005). Thus, for example, during the "Defense Meteorological Satellite Program" (DMSP), satellites observed strong irregular density troughs related to SAPSWS's, which coincided well with signal scintillation events (Basu et al., 2001; Ledvina et al., 2002).

Within troughs, the power spectral density (PSD) denoted by $S(k)$ was well-approximated by the plasma density power law $(\delta n_k/n_0)^2 \sim k^{-p}$ with the spectral index ranging in the limits $5/3 < p \leq 2$ (Mishin and Blaunstein, 2008). In this case, it was taken into account that disturbances of plasma density δn_k can achieve 10–20% with respect to nonperturbed ionospheric plasma (Mishin and Blaunstein, 2008) in a

range of apparent wave numbers from $k = 2\pi/\lambda = 0.85\ \text{km}^{-1}$ to $k = 12\ \text{km}^{-1}$, where λ is the wavelength.

In all derivations of the formulas presented in (Mishin and Blaunstein, 2008), it was stated from the beginning that the considered perturbed plasma is quasi-neutral and the magnitudes of disturbances of the electron and ion components are equal to each other.

The spectral properties of plasma perturbations allow for predicting the spectral characteristics of a radio signal on the basis of data (called the bandpass signal (Blaunstein, 2004)) and, finally, the type of fading (flat or frequency-selective) in such a type of perturbed ionospheric channel. These aspects are very real for advanced wireless networks, designed based on modern technologies of signal processing, namely, orthogonal frequency division multiplexing (OFDM), where each subscriber obtains a very narrow bandwidth. The main goal for such a technique is to eliminate the effects of the noise caused by the multipath propagation phenomenon occurring in a channel with fading and multichannel interference (Blaunstein and Christodoulou, 2007).

Therefore, it is important to predict a priory the type of a channel and the frequency or time of spreading (or both characteristics) for the evaluation of the coherent throughput and time of coherency of such a channel with fading to ensure future access to special technologies for networks based on the OFDM technique (Blaunstein and Christodoulou, 2007). The above-mentioned examples show the actuality of this work and the investigations carried out in it.

The paper describes the phenomenon of fading and its effects on key parameters of radio signals in the land–satellite channel passing through stratified ionospheric plasma, perturbed by a magnetic storm and filled with "typical" small and moderate irregularities. The basic effects of irregular plasma structures, embedded within SAPS's, defined by the propagation of radiowave signals through a perturbed ionosphere, are briefly discussed in Section 2. In Section 3, we present the results of a computation of the integral absorption of a signal, deviations of the amplitude and phase in a "point-to-point" channel, and variations in the intensity and phase of radio signals propagating through this SAPSWS-related "typical" radio link. These results help to understand the effects of fading phenomena on signals passing through the ionosphere with multipath propagation during magnetic storms. In conclusion, the main effects of radio signals of various frequency bands propagating in a perturbed ionosphere during magnetic storms are summarized.

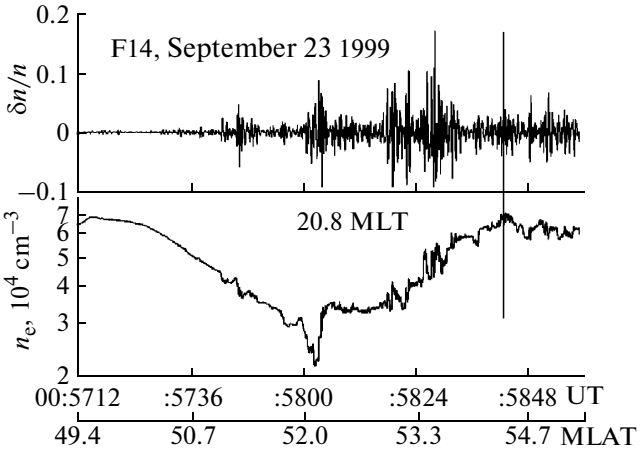

Fig. 1. Observations on the DMSP F14 satellite during the magnetic storm of September 23, 1999, Boston, Massachusetts, United States. The top panel shows a waveform of relative density variations $\delta n/n_0$; the bottom panel, the density variation along the satellite track.

2. SATELLITE OBSERVATIONS OF INHOMOGENEITIES OF PLASMA CONCENTRATION RELATED TO SAPS PHENOMENA

Figure 1 (data from (Mishin and Blaunstein, 2008) is used) presents the parameters of the plasma registered by the DMSP F14 satellite near a scintillation event near Boston, MA, United States, during the magnetic storm of September 23, 1999 (Basu et al., 2001). Shown in the bottom panel is the plasma density variation along the satellite track measured by a spherical Langmuir probe sampled at a rate of 24 Hz. A detailed description of the probe and the whole DMSP/SSIES project can be found in (Hardy et al., 1984; Rich and Hairston, 1994; Maynard et al., 1996; Foster and Rich, 1998). It is seen that the satellite moved in the region of the main trough, which was shifted southward at more than 7 deg relative to its nonperturbed position (~60 MLAT).

The top panel shows the corresponding waveform of plasma density deviations $\delta n/n_0$ obtained by applying a bandpass elliptic filter with a band of 0.1–9.5 Hz (a more detailed description can be found in (Basu et al., 2001)). Here δn is the perturbation of the ionosphere with respect to the nondisturbed background plasma density (denoted by n_0). As can be seen, enhancement of small-scale plasma density fluctuations appeared near the equatorial boundary of the polar cups (indicated by a vertical line); that is, beyond the limits of the main trough, the sub-auroral ionosphere was also perturbed.

For example, we present now other perturbed subauroral inhomogenetities of the plasma concentration, which were observed by the DMSP F13 and F15 satellites during a magnetic storm on March 31, 2001 (Ledvina et al., 2002). In Fig. 2, variations in the hor-

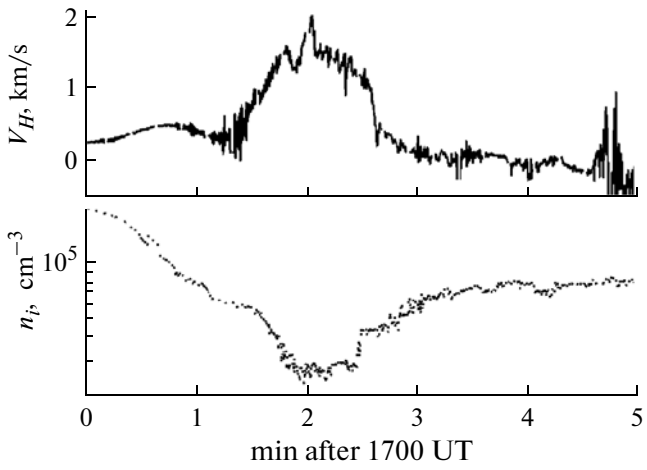

Fig. 2. Horizontal (positive westward) component V_H of the convection velocity in km/s (top panel) and plasma density from the DMSP F15 satellite on March 31, 2001 (bottom panel) (according to the materials from (Ledvina et al., 2002)).

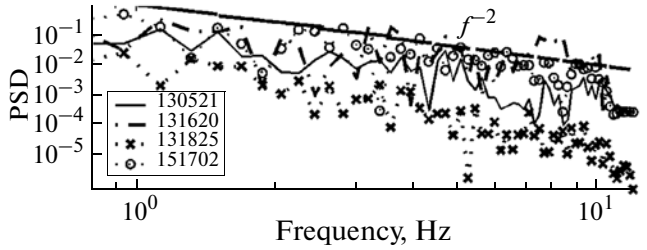

Fig. 3. Power spectral density of plasma irregularity relative to the apparent frequency obtained from the DMSP satellites for various time periods. 130521 is the F13 satellite at 0521 UT, etc. (according to the data from (Mishin and Blaunstein, 2008)).

izontal (positive westward) component of convection velocity V_H (the top panel) and plasma density n_i (bottom panel), obtained from the F15 satellite with the help of a ion drift meter and a Langmuir probe with a sampling rate of 6 and 24 Hz, respectively.

It should be noted that quite similar SAPS (trough) structures were also observed throughout the storm by the DMSP F13 satellite. As in (Basu et al., 2001; Ledvina et al., 2002; Mishin and Blaunstein, 2008; Foster and Rich, 1998), we obtain waveforms of variations in the plasma density in the SAPS regions applying a 0.1–9.5 Hz bandpass elliptic filter. The PSD is shown in Fig. 3 as a function of the apparent frequency. Moreover, in (Basu et al., 2001; Ledvina et al., 2002; Erickson et al., 2002; Foster and Burke, 2002; Mishin et al., 2003; Mishin and Burke, 2005; Pfaff et al., 2008; Mishin and Blaunstein, 2008), the PSD is well represented by the law $\delta n_k/n_0 \propto k^{-p}$, $p = 2$ (or $\delta n_f/n_0 \propto f^{-2}$), where $k = 2\pi f/c$ and p is the PSD parameter.

It should be emphasized that, based on the data of a single satellite, the separation of spatial and temporal variations is impossible and, therefore, the frequencies (wavelengths) seem to be apparent frequencies (spatial scales). Given the satellite speed $v_s = 7.5$ km/s, apparent frequencies of 1–10 Hz correspond to wavelengths $\lambda_s = 2\pi/k_s = v_s/f = 7.5$–$0.75$ km along the satellite track. It should be noted that after about 1900 UT the short-scale oscillations decay, whereas "smooth" SAPS/trough plasma structures remain throughout even after the magnetic storm recovery phase. Such behavior is typical of SAPSWS's, which are developed within 10–20 min and decay ~1 an hour after the beginning of the explosive phase of a magnetic storm (Foster and Burke, 2002; Mishin and Burke, 2005; Mishin and Blaunstein, 2008).

3. KEY PARAMETERS OF RADIO SIGNALS AND PROPAGATION CHANNEL

3.1. Key Parameters of a Radio Channel

In the process of prediction, the key parameters of a radio channel passing through the irregular ionosphere will be characterized by the spectral index $p = 1 + \langle n \rangle$, ($\langle n \rangle$ is the mean value of the plasma refractive index) or by the PSD index $p' = p - 2$ (Booker and Gordon, 1950; Booker et al., 1950; Booker, 1956; Booker and Majidi Ahi, 1981; Booker, 1981; Farley, 1996; Blaunstein and Christodoulou, 2007; Blaunstein and Plohotniuc, 2008). It is also important to mention that the signal intensity fluctuations at a given frequency can be described by the Ricean K-parameter as a ratio of the coherent and incoherent components of the total signal intensity (Blaunstein, 2004):

$$K = \langle I_{co} \rangle / \langle I_{inc} \rangle. \tag{1}$$

Here $\langle I_{co} \rangle$ is the component of a signal propagating under the conditions of direct visibility (line of sight, LOS), also called the coherent part (Saunders, 1999; Blaunstein, 2004; Blaunstein and Christodoulou, 2007), and $\langle I_{inc} \rangle$ is the incoherent component of the total signal intensity

$$\langle I \rangle = \langle I_{co} \rangle + \langle I_{inc} \rangle, \tag{2a}$$

where

$$\langle I_{inc} \rangle = \langle I_{co} \rangle \sqrt{\sigma_I^2}. \tag{2b}$$

The scintillation index of signal intensity I is

$$\sigma_I^2 = \frac{\langle I^2 \rangle - \langle I \rangle^2}{\langle I \rangle^2} = \frac{\langle I^2 \rangle}{\langle I \rangle^2} - 1, \tag{2c}$$

usually denoted as S_4 in literature (Basu et al., 2001; Ledivina et al., 2002; Erickson et al., 2002; Foster and Burke, 2002; Mishin et al., 2003; Mishin and Burke, 2005; Kintner and Ledivina, 2005; Pfaff et al., 2008; Mishin and Blaunstein, 2008) . This index defines the normalized value of a fast-fluctuating signal (i.e., of fast signal fading).

For the amplitudes of the Gaussian zero-mean random signal, the relationship between K and σ_I^2 (denoted as S_4 in this work) is simply written as

$$K^2 = 1/\sigma_I^2 \equiv 1/S_4. \quad (3)$$

It should be noted that, according to (Blaunstein and Christodoulou, 2007), for a Gaussian random signal with a nonzero mean value, from relationships (1)–(2c), it is clearly seen that formula (3) becomes more complicated. However, as was shown by many researchers who studied stochastic processes in a perturbed ionosphere (Backley, 1971; Titheridge, 1971; Crain et al., 1974; Wernik and Liu, 1975; Rino and Fremouw, 1977; Booker, 1981; Rino, 1982; Knepp, 1983; Blaunstein and Christodoulou, 2007), the spatial distribution of natural and artificially generated ionospheric inhomogeneities can be correctly described by the law for a Gaussian random signal with a zero mean value, which, according to the ergodic theorem, yields the same Gaussian distributions of scattered radio signals in the time domain.

The basic characteristics of a signal with fading can be derived by using the approaches developed in (Denisov and Erukhimov, 1966; Erukhimov and Rizhkov, 1971; Backley, 1971; Titheridge, 1971; Crain et al., 1974; Wernik and Liu, 1975; Rino and Fremouw, 1977; Erukhimov et al., 1980; Booker, 1981; 1982; Ga'lit et al., 1983; Knepp, 1983) and summarized in (Blaunstein and Christodoulou, 2007; Blaunstein and Plohotniuc, 2008). They are as follows:

(1) Mean square phase fluctuation $\left\langle (\Delta\Phi)^2 \right\rangle$,

(2) Outer scale L_0 of the disturbed ionospheric plasma structure.

(3) Inner scale l_0 of a plasma density inhomogeneity.

In addition, to describe radiowave propagation in perturbed plasmas, outer scale L_0 should be of the same order as the Fresnel scale $d_F = \sqrt{\lambda Z_0}$ (Gurevich and Tsedilina, 1979; Ge'berg, 1986; Blaunstein and Plohotniuc, 2008). Here λ is the wavelength of the signal and Z_0 is the distance from the ionospheric layer filled with plasma inhomogeneities to the plane of signal reception at the ground surface (Erukhimov and Rizhkov, 1971; Gurevich and Tsedilina, 1979; Erukhimov et al., 1980; Ga'lit et al., 1983; Blaunstein and Christodoulou, 2007).

The spectrum of signal intensity fluctuations can be derived by using the root mean square (RMS) of phase fluctuations $\sqrt{\left\langle (\Delta\Phi)^2 \right\rangle}$ (Rino and Fremouw, 1977; Rino, 1982; Deminov et al., 1999; Blaunstein and Plohotniuc, 2008) by assuming that the RMS of phase fluctuations is larger than one radian. Moreover, in (Booker, 1956; Crain et al., 1974; Booker and Majidi Ahi, 1981; Blaunstein and Christodoulou, 2007; Blaunstein and Plohotniuc, 2008), it was shown theoretically that for $k \gg 1/L_0$ the power spectrum of phase fluctuations $S(k)$ in a perturbed inhomogeneous ionosphere is proportional to k^{-p} (e.g., f^{-p}), where $p = 2$ (see Fig. 3). This relationship was proved by numerous observations in a perturbed ionosphere (see, for example (Deminov et al., 1999; Mishin and Blaunstein, 2008)).

3.2. Main Characteristics of Signal Fading

We analyze the propagation characteristics of a radiowave passing through an inhomogeneous ionospheric region, perturbed by a geomagnetic storm. As it follows from the experimental data presented above, the background ionospheric plasma can be essentially perturbed during the preparation period of a magnetic storm. Observations during this period have shown that plasma density, relative to its undisturbed background, can achieve 10–20% (see Figs. 1, 2). There are several signal characteristics that should be evaluated for the prediction of fading phenomena in satellite communication links passing through a perturbed ionosphere, such as absorption, attenuation of a signal along the transmitter–receiver radio path, phase variations in the radio signal along the trace, as well as scattering effects that cause signal intensity variations and random phase deviations.

3.2.1. Absorption of radio signals in a perturbed ionosphere. To estimate the losses related to the absorption phenomenon, that is, the part of the energy of a radiowave which is absorbed in the perturbed region of the ionosphere (from the D to the F region), following (Gurevich and Tsedilina, 1979; Blaunstein and Christodoulou, 2007; Blaunstein and Plohotniuc, 2008), we propose here to use special magnitudes of absorption in decibels (dB):

$$A_\omega = 10\log\frac{I_0}{I} \approx \frac{4.3}{c}\int \frac{\omega_{pe}^2(\nu_{em}+\nu_{ei}+\nu_{ee})}{\left[\omega^2+(\nu_{em}+\nu_{ei}+\nu_{ee})^2\right]}ds, \quad (4)$$

where ν_{em}, ν_{ei}, ν_{ee}, and are the frequencies of electron–neutral, electron–ion, and electron–electron collisions, respectively.

The absorption parameter fully characterizes real ionospheric radio propagation traces and, as a rule, is estimated by measuring radiometric absorption at fixed frequencies and by knowledge of the frequency dependence of the coefficient of absorption κ. It should be noted that in the integrand of expression (4) we not only took into account the effects of electron–neutral and electron–ion collisions, but also ion–neutral and electron–electron collisions based on elements of kinetic theory (Kadomtsev, 1965; Shkarofsky et al., 1966; Tsytovich, 1970; Gurevich, 1978), but not of the magnetoionic theory, usually used in such derivations based on classical hydromagnetic approaches.

Thus, deriving A_ω, taking into account relationship (4) for the length of radio path s and the height of the ionosphere h, we get $h = s \cdot \sin\psi$, where ψ is the angle

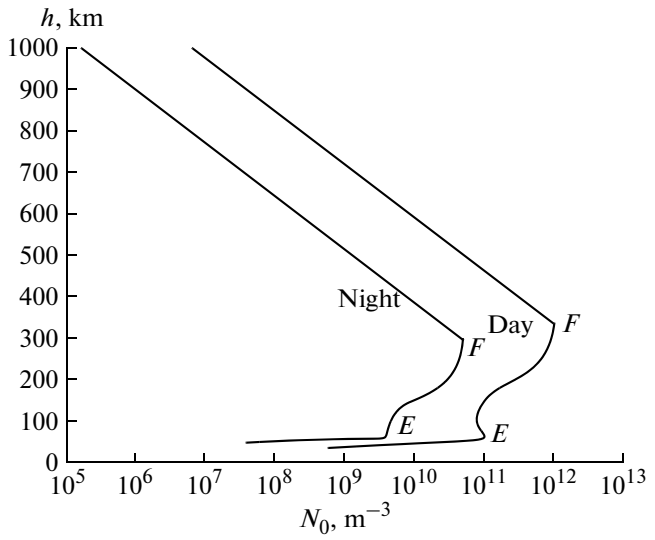

Fig. 4. Profile of $N_0(h)$ during moderate solar activity according to published data (Deminov et al., 1995; Blaunstein and Plohotniuc, 2008).

of inclination of the satellite antenna with respect to the ground-based antenna (called the grazing angle); it is possible to evaluate the total absorption of a radio signal along the path. In Figs. 5–7, this parameter is presented in decibels vs. the carrier frequency of probing radio signal propagating through a perturbed ionosphere under different grazing angles, respectively. The corresponding profiles of disturbed plasma density were taken from Figs. 1 and 2. (More detailed information on perturbations of the total plasma content in a perturbed ionosphere can be found in (Basu et al., 2001; Ledivina et al., 2002; Pfaff et al., 2008; Mishin and Blaunstein, 2008).)

The corresponding magnitudes of the full density of disturbed plasma were normalized on vertical profiles of electron concentration and are shown in Fig. 4 according to the conclusions made in (Deminov et al., 1995; Blaunstein and Plohotniuc, 2008) for an unperturbed midlatitude daytime and nocturnal ionosphere. Computations of integral (4) were made for $h_{\min} = 50$ km and $h_{\max} = 500$ km.

We consider below two scenarios of a weak (Mishin and Blaunstein, 2008) and strong (Pfaff et al., 2008) magnetic storms, which are presented in Figs. 5–7.

As follows from the presented illustrations, with an increase in the magnetic storm strength (from weak in Figs. 5a, 6a, and 7a to strong in Figs. 5b, 6b, and 7b), absorption of radio signals increases sharply by three times at lower frequencies from 100 to 500 MHz, while at 500–600 MHz absorption does not depend on the frequency as it only depends on the grazing angle. At the same time, with an increase in the grazing angle, a tendency towards an decrease in signal absorption by two to three times is evident for weak magnetic storms as compared to strong storms. The computation results presented above allow for the conclusion that magnetic storms occurring in the northern and middle latitudes of the ionosphere can significantly perturb ionospheric plasma and cause sharp attenuation of radio signals up to 500 MHz. This effect depends on the grazing angle and can be insignificant for angles larger than $\psi \geq 20°$. Therefore, with an increase in the radiating frequency of radio signals for the same grazing angle or with an increase in grazing angle for the same frequency, a tendency towards insignificant absorption of signal energy is evident.

3.2.2. Signal amplitude "point-to-point" attenuation and signal phase deviations. It should be pointed out that for radio communication and radars other characteristics of signal fading can give information on physical radio effects, dealing not with the cumulative intensity of integral absorption along a radio path, but with the "point-to-point" amplitude and phase deviations of any wave along that path. In this case, it is important to understand how the perturbed parameters of the ionospheric plasma decrease the amplitude of a radiowave and change its phase. To understand these radiophysical effects, we will consider an arbitrary monochromatic radiowave (Blaunstein and Christodoulou, 2007; Blaunstein and Plohotniuc, 2008):

$$U(z,t) = A(z,t)\exp[i(\omega t - kz)]. \quad (5)$$

In this case, complex wave k can be described through the coefficient of wave amplitude attenuation α and the coefficient determining changes in the wave phase in real time β; i.e.,

$$k = \alpha + i\beta. \quad (6)$$

Unlike the usual description of parameters α and β, we will present them through the frequencies of collisions of plasma particles using elements of kinetic theory (see (Deminov et al., 1995; Blaunstein and Plohotniuc, 2008)) For numerical computations, we introduce additional notations and parameters to describe α and β, such as $X = \omega_p^2/\omega^2$ and $Z = \nu/\omega$, where ω_p is the background plasma frequency in a perturbed ionosphere (Blaunstein and Plohotniuc, 2008). Using these notations, we got

$$k^2 = \frac{\omega^2}{c^2}\left[1 - \frac{X}{1 - iZ}\right] = \frac{\omega^2}{c^2}\left[1 - \frac{X(1+iZ)}{1+Z^2}\right] = \frac{\omega^2}{c^2}\left[1 - \frac{X + iZX)}{1+Z^2}\right], \quad (7a)$$

or

$$k^2 = \frac{\omega^2}{c^2}\left[1 - \frac{X}{1+Z^2} - i\frac{ZX}{1+Z^2}\right]. \quad (7b)$$

By introducing now the normalized parameters (to the wave number in free space k_0), $\tilde{\alpha} = \dfrac{\alpha}{k_0}$ and $\tilde{\beta} = \dfrac{\beta}{k_0}$, we finally get

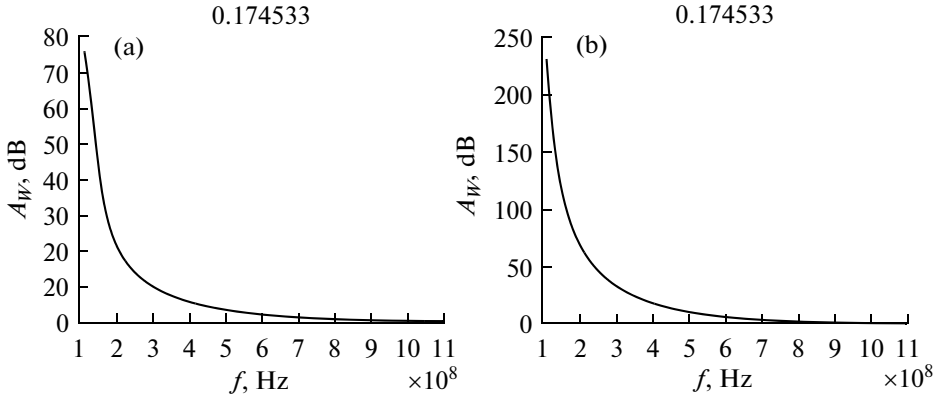

Fig. 5. Absorption of a signal (dB) vs. frequency for $\psi \approx 0.175$ rad or $\psi \approx 10°$: (a) weak magnetic storm and (b) strong magnetic storm. The results are presented for a region in the North of the United States (Alaska).

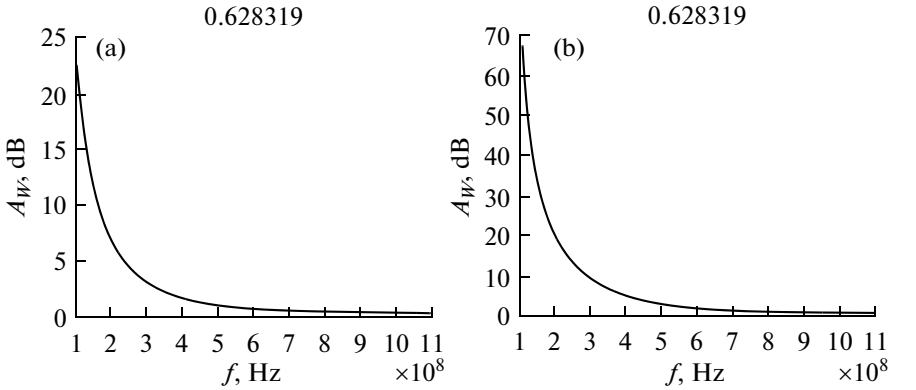

Fig. 6. Absorption of a signal (dB) vs. frequency for $\psi \approx 0.628$ rad or $\psi \approx 36°$; (a) weak magnetic storm and (b) strong magnetic storm.

$$\tilde{\alpha} = \frac{1 + \left(\frac{\nu}{\omega}\right)^2 - \frac{\omega_p^2}{\omega^2}}{1 + \left(\frac{\nu}{\omega}\right)^2} = \frac{\omega^2 + \nu^2 - \omega_p^2}{\omega^2 + \nu^2}, \tag{8a}$$

$$\tilde{\beta} = \frac{ZX}{1 + Z^2} = \frac{\left(\frac{\nu}{\omega}\right)\frac{\omega_p^2}{\omega^2}}{1 + \left(\frac{\nu}{\omega}\right)^2} = \frac{\nu\omega_p^2}{\omega\left(\omega^2 + \nu^2\right)}, \tag{8b}$$

here $\nu = \nu_{em} + \nu_{ei} + \nu_{ee} = \nu_{em}(1 + q + q')$;, where $q = \nu_{ei}/\nu_{em}$; and $q' = \nu_{ee}/\nu_{em}$.

Deviations of the parameters of the radio signal and in the perturbed ionospheric region, were obtained with help of parameters of the perturbed ionosphere, ω_p/ω_{p0}; i.e., of deviation of plasma frequency; plasma concentration N/N_0, $N = N_0 + \delta N$, $\delta N < N_0$; σ is the plasma conductivity, N_0, and σ_0 are the parameters of the background non-disturbed ionosphere (Blaunstein and Plohotniuc, 2008):

$$\omega_{p0} = \left(4\pi N_0 e^2/m_e\right)^{1/2}, \tag{9}$$

$$\varepsilon_0 = 1 - \left[\omega_0^2/\left(\omega^2 + (\nu_{em} + \nu_{ei})^2\right)\right], \tag{10}$$

$$\sigma_0 = \left[\omega_0^2(\nu_{em} + \nu_{ei})/4\pi\left(\omega^2 + (\nu_{em} + \nu_{ei})^2\right)\right]. \tag{11}$$

Here e and m_e are the charge and mass of plasma electrons; other parameters are defined above. In Figs. 8 and 9, deviations of parameters α and β of radio signals, compared to magnitudes α_0 and β_0 obtained for undisturbed ionospheric plasma, are shown. The results of computations for normalized attenuation are shown in Fig 8 (for the normalized phase velocity, in Fig. 9), depending on the altitude of the ionosphere for different frequencies of probing radiowaves, varying in a range from 50 MHz to 2 GHz (i.e., also covering the HF band, which is relevant for the transionospheric propagation of radiowaves).

Hence, we use those frequencies in computations which are actual in applications of navigation of land–ionosphere–land traces ($f < 500$–600 MHz), as well as in usually used radio monitoring of the ionosphere by signals of GPS/GLONASS ($f > 900$ MHz).

As seen from Fig. 8, with increasing frequency of a probing radiowave, the effect of attenuation of the

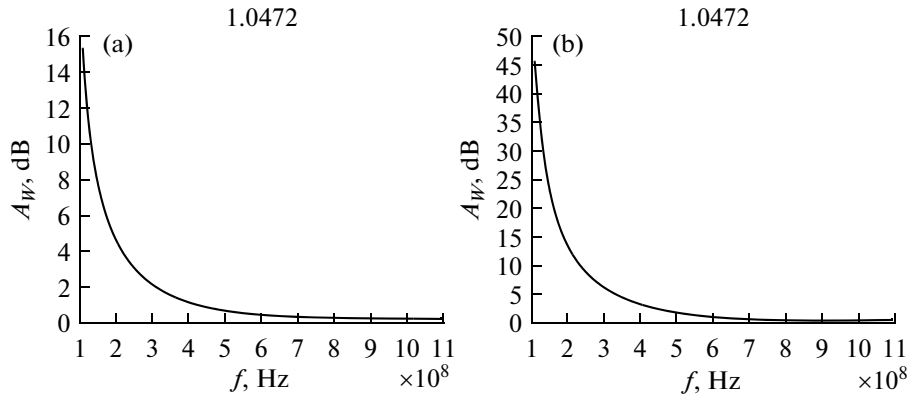

Fig. 7. Absorption of a signal (dB) vs. frequency for $\psi \approx 1.05$ rad or $\psi = 60°$; (a) weak magnetic storm and (b) strong magnetic storm.

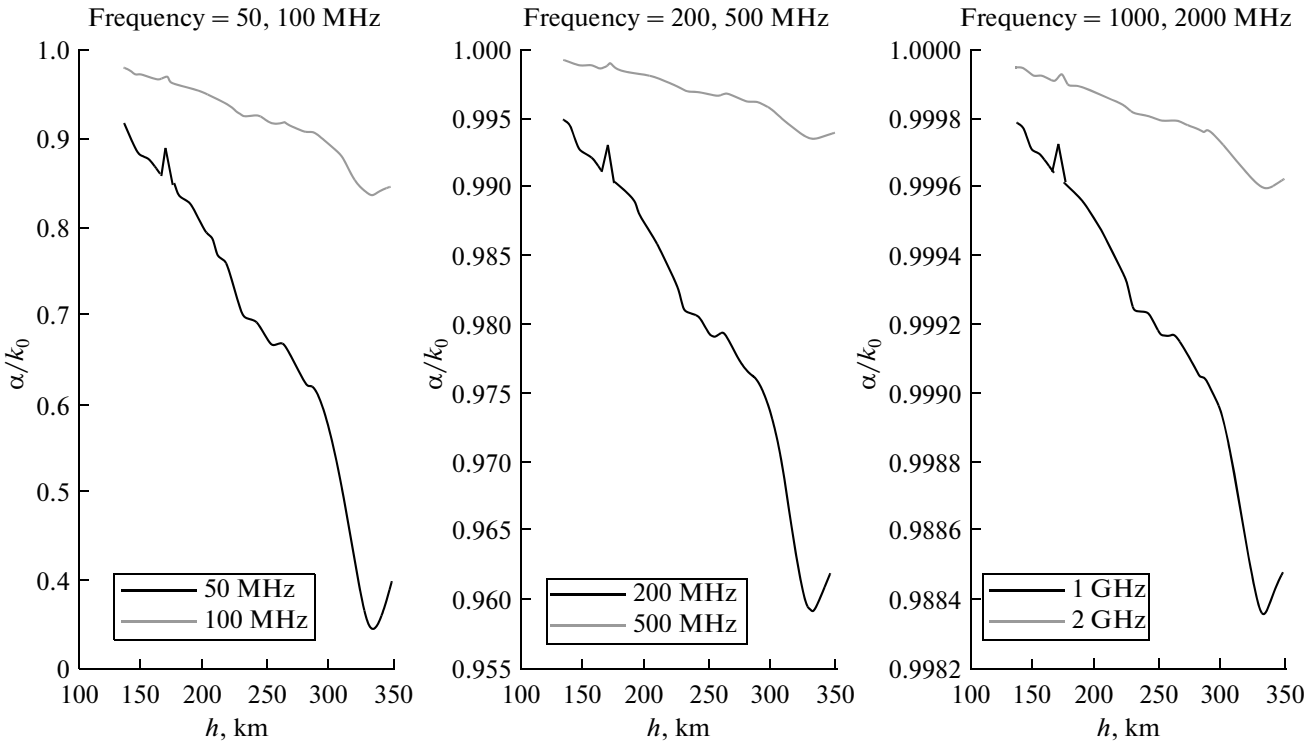

Fig. 8. Calculation results of normalized attenuation coefficient α vs. ionospheric altitudes for different frequencies of probing waves: from 50 MHz to 2 GHz.

wave energy becomes weaker and the probing radiowaves propagate similarly as in an undisturbed ionosphere. This effect depends strongly on the altitudes at which a radiowave propagates. Estimations show that with an increase in the ionospheric altitude, the effect of attenuation is also increased for all working frequencies under consideration.

In Fig. 9, a tendency is clearly observed towards a decrease in the phase velocity of the radiowave passing through the disturbed ionospheric region with an increase in the frequency of the probing wave from 50 MHz to 2 GHz; that is, the phase velocity of the probing wave becomes smaller in disturbed plasma comparing to that in undisturbed plasma.

This effect can be easily explained. When the frequency increases (or the wavelength decreases compared to the dimensions of plasma irregularities), the effect of "diffractive scattering" becomes weaker, and

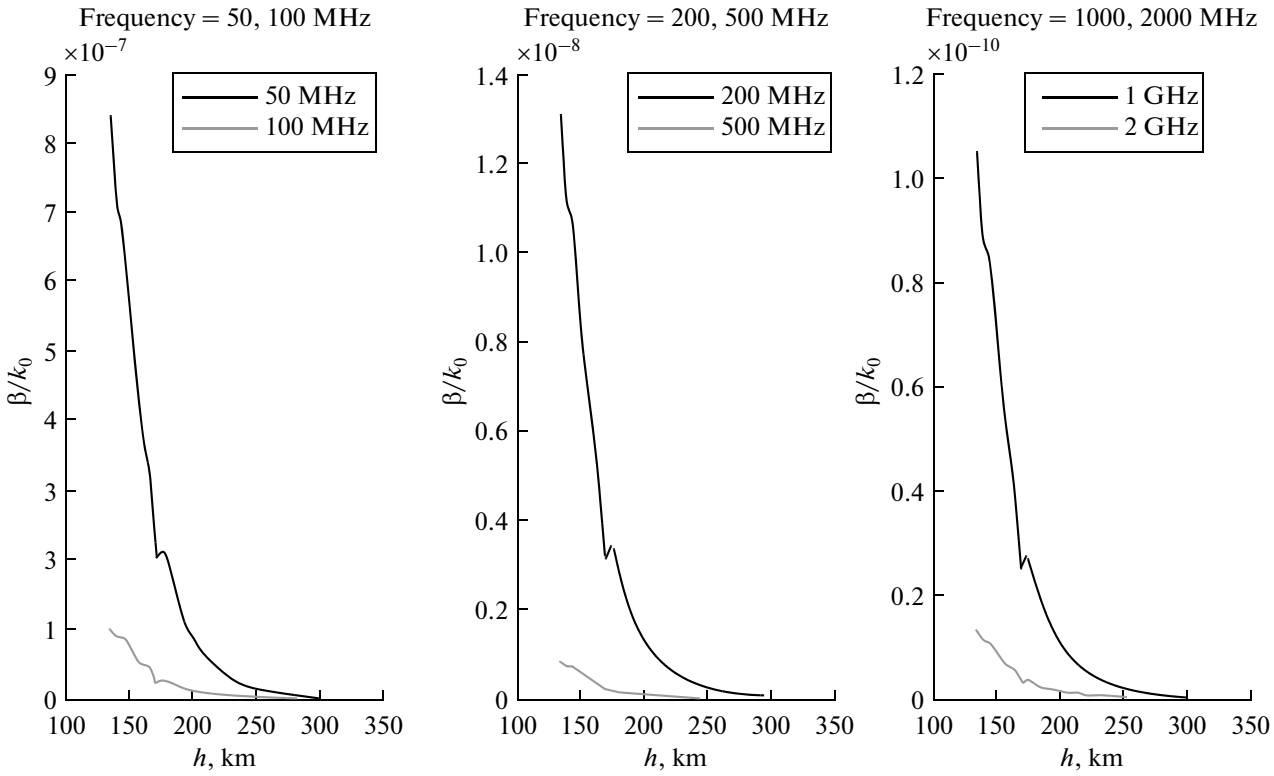

Fig. 9. Calculation results of normalized phase velocity β vs. ionospheric altitudes for different frequencies of probing waves:from 50 MHz to 2 GHz.

instead of a defocusing effect with strong fading we observe a focusing effect with weak fading (Blaunstein and Christodoulou, 2007; Blaunstein and Plohotniuc, 2008).

3.2.3. Signal intensity fluctuations. For the investigation of signal intensity fluctuations in a perturbed ionosphere and the corresponding evaluation of the scintillation index for ionospheric models with plane (Booker and Gordon, 1950; Booker at el., 1950; Booker, 1956; Booker and Majidi Ahi, 1981; Booker, 1981; Rino, 1982; Knepp, 1983; Farley, 1996) and curved (Erukhimov at el., 1980; Ga'lit at el., 1983) reflected surface, computations were carried out which were later summarized in (Blaunstein and Christodoulou, 2007; Blaunstein and Plohotniuc, 2008).

In the framework of the theoretical self-consistent concept described in the work, it is possible to estimate the effects of a magnetic storm based on variations in the two above-mentioned parameters of radio signals propagating in a perturbed ionospheric communication channel. Thus, only for the conditions of a magnetic storm, described by the PDS parameter $p = 4$ ($p' = 2$), introduced in Section 2 (see Fig. 3), we finally get the following (Blaunstein and Christodoulou, 2007; Blaunstein and Plohotniuc, 2008):

$$I(k) = 32\left\langle(\Delta\Phi)^2\right\rangle \frac{L_0}{\left(1+k^2L_0^2\right)^2}\sin^2\left(\frac{1}{2}k^2d_F^2\right). \qquad (12)$$

In the framework of the self-consistent model described in (Blaunstein and Christodoulou, 2007; Blaunstein and Plohotniuc, 2008) for various scenarios occurring in a strongly perturbed ionosphere, for $p' = 2$ ($p = 4$), we get the following expression of the scintillation index:

$$\sigma_I^2 = \frac{8\sqrt{2}}{3\sqrt{\pi}L_0^3} d_F^3 \left\langle(\Delta\Phi)^2\right\rangle. \qquad (13)$$

Computations of the scintillation index presented by formula (13) were compared in (Blaunstein and Christodoulou, 2007; Blaunstein and Plohotniuc, 2008) with the expressions obtained in (Booker and Gordon, 1950; Booker at el., 1950; Booker, 1956; Booker and Majidi Ahi, 1981; Booker, 1981; Rino, 1982; Knepp, 1983) for weak and moderate plasma perturbations (for example, for $p = 2$ ($p' = 0$) and $p = 3$ ($p = 1$), respectively), for the outer scale $L_0 = 10d_F$ and inner scale $l_0 = 10^{-2}d_F$. In Figs. 10a and 10b, the RMS

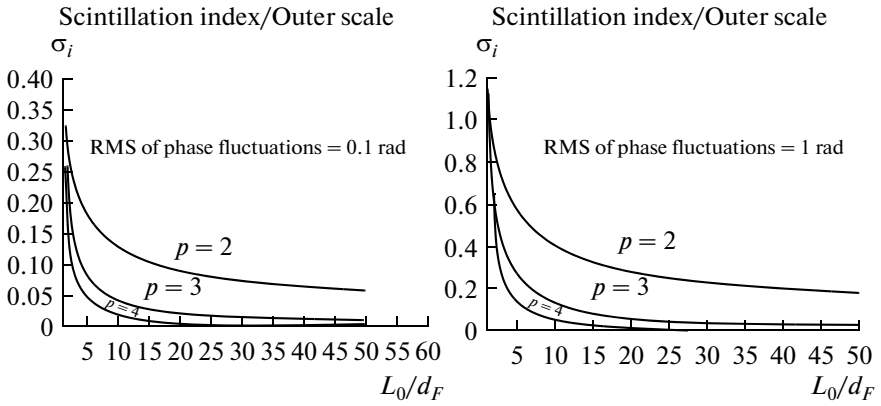

Fig. 10. RMS of the scintillation index vs. outer scale L_0 for $1.5d_F \le L_0 \le 50d_F$: $\sqrt{\left\langle (\Delta\Phi)^2 \right\rangle}$ = (a) 0.1 and (b) 1 rad.

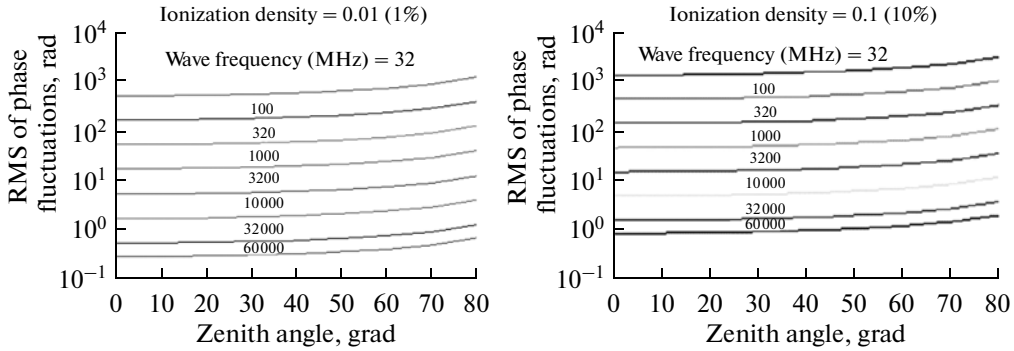

Fig. 11. RMS of signal phase fluctuation $\sqrt{\left\langle (\Delta\Phi)^2 \right\rangle}$ (in radians) vs. zenith angle of the satellite: (a) for $\delta N/N_0 = 0.01$ and for frequencies from 32 MHz to 60 GHz; (b) for $\delta N/N_0 = 0.1$.

of the scintillation index $\sigma_I \equiv \sqrt{\sigma_I^2}$, computed for weak ($\sqrt{\left\langle (\Delta\Phi)^2 \right\rangle} = 0.1$ rad) and moderate ($\sqrt{\left\langle (\Delta\Phi)^2 \right\rangle} = 1$ rad) phase fluctuations are shown, compared to the mean-square value of the phase deviation for various PDS parameters (p = 2, 3, and 4) and for different scales of ionospheric irregularities.

It is seen that for $p = 2$ the scintillation index tends to 1 with increasing phase fluctuations. In the latter case, for higher magnitudes of the spectral index ($p > 2$), σ_I exceeds 1 within the range $0 < L_0/d_F < 1$, which explains the focusing properties of the ionospheric layer containing various irregularities and strong variations in the signal phase after passing the perturbed ionosphere.

3.2.4. Signal Phase Fluctuations. We modeled the ionospheric F region, according to the method discussed in (Deminov et al., 1995; Blaunstein and Plohotniuc, 2008), as a spherical three-dimensional layer with mean plasma concentration N, outer scale L_0 (instead of a plane-layer one-dimensional model, as was done in (Booker and Gordon, 1950; Booker at el., 1950; Booker, 1956; Booker and Majidi Ahi, 1981; Booker, 1981; Rino, 1982; Knepp, 1983; Farley, 1996)), and with the standard fluctuations of concentration $(\Delta N/N_0)^2 \equiv (\delta N/N_0)^2$.. We assume outer scale L_0 to be equal to the thickness of the disturbed ionospheric F region. In such notations, the mean square magnitude of phase fluctuations of radio signals can be derived by using a general model (Deminov et al., 1995; Blaunstein and Christodoulou, 2007; Blaunstein and Plohotniuc, 2008), which finally gives

$$\left\langle (\Delta\Phi)^2 \right\rangle = 4r_e^2 N_0^2 \left\langle \left(\frac{\delta N}{N_0} \right)^2 \right\rangle \lambda^2 H^2 \sec\chi. \qquad (14)$$

Here, r_e is the radius of an electron. For numerical computations, we take $H = 100$ km and $N_0 = 10^{11}$ m^{-3}. In Figs. 11a and 11b, the RMS of the signal phase fluctuations, $\sqrt{\left\langle (\Delta\Phi)^2 \right\rangle}$ (in radians), is shown, depending on the zenith angle of a satellite for various frequencies from 32 MHz (HF band) to 60 GHz (UHF band) and for different $\delta N/N_0$ in percentages in respect to the

Main effects of radio propagation during a magnetic storm

Phenomenon	Effects of a magnetic storm
Plasma density variations	Weak storm, $\delta n/n_0 = 2–5\%$. Strong storm, $\delta n/n_0 = 10–20\%$.
Attenuation	Threefold change from a weak magnetic storm to a strong one (see Figs. 5–7). Changes do not depend on the grazing angle. At the same time, with a decrease in the grazing angle for frequencies up to 600 MHz, attenuation of the radio signal increases.
Phase fluctuation	From tens to hundreds of radians with an increase in the magnetic storm intensity (see Fig. 11).
Scintillation index variations	From 0.4 to 0.8 (for $p = 2$) with respect to the nonperturbed ionosphere (see Fig. 10).
Criterion of fast fading	$K \in [0.8–1.6]$; I_{co} is at the same order or slightly higher than I_{inc}. For a description of such radio channels, the Ricean law can be used.

mean plasma concentration at $N_0 = 10^{11}$ m^{-3} from 1 (a weak magnetic storm) to 10% (a strong magnetic storm), respectively.

Here, we should notice that the frequency band of signals that we investigate covers the entire spectra of the useful frequencies operating in the land–ionosphere–land communication link, GPS/GLONASS, as well as in new networks of the next fourth generation, operating at frequencies from 10 GHz to 60 GHz. As is clearly seen from the presented frequency dependences, the RMS of signal phase fluctuations have essential magnitudes only for zenith angles greater than 60°–65° for moderate and large perturbations of the background ionospheric plasma, i.e., from 1 to 10%.

With an increase in the wave frequency, phase fluctuations become strongly depending on $\delta N/N_0$. Thus, for a frequency band from 1 to 10 GHz, usually used in satellite communications for zenith angles of 50°–60°, the RMS of phase fluctuations increases from 1–5 to 20 rad ($\delta N/N_0 = 0.01$), achieving up to 100 rad ($\delta N/N_0 = 0.1$).

3.2.5. Effects of fast fading on a radio signal. Based on the effects of a magnetic storm, experimentally observed during sounding of a disturbed ionosphere, we will analyze the effects of fading on radio signals, which are determined by the K-parameter of fading, described in Section 3.1.

For these purpose, we will use the relationship between the parameter of signal intensity scintillations σ_I^2 and the K-parameter described by formula (3), as a criterion of fast fading within a channel (Blaunstein and Christodoulou, 2007; Blaunstein and Plohotniuc, 2008). Taking into account the experimentally observed (Basu et al., 2001; Ledvina et al., 2002; Kintner and Ledvina, 2005) variations in the scintillation index $S_4 \equiv \sigma_I^2$, ranging from 0.4 to 0.8 (see also Figs. 1 and 2 in Section 2), we get that the corresponding K-parameter varies from 1.1 to 1.6, indicating the existence of direct visibility between the ground-based and satellite antennas. From the above-presented examples, it is seen that a signal in direct propagation has the same order or higher than that in the case of absence of direct visibility. In other words, the coherent component of signal intensity is complimented by the effects of multipath propagation (i.e., by the incoherent component), caused by diffractive scattering of radio signals on small- and medium-scale inhomogeneities of plasma density $\delta N/N_0$, which exist in a perturbed ionosphere (see Figs. 1–3). Changes in the K-parameter within a range from 1.1 to 1.6 imply that the coherent component under the conditions of direct visibility exceeds the incoherent component (non-line-of-sight propagation) even in a perturbed ionosphere. As was shown in (Blaunstein and Christodoulou, 2007; Blaunstein and Plohotniuc, 2008), knowing the K-parameter of fast fading, it is possible to predict deviations of the parameters of a signal passing through a disturbed ionospheric radio channel, such as the spectral efficiency and the number of errors of digital signals (bit error rate, BER).

4. CONCLUSIONS

Theoretical computations of the intensity and phase fluctuations of radio signals propagating in a stormtime subauroral and midlatitude ionosphere have been presented. The main ionospheric parameters and the parameters of plasma irregularities used in the computations were taken from the DMSP satellite observations during magnetic storms. Indeed, two events were considered when intensive scintillations of radio signals were observed during a magnetic storm (see Section 2 and the corresponding references in (Basu et al., 2001; Ledivina et al., 2002; Erickson et al., 2002; Foster and Burke, 2002; Mishin et al., 2003; Kintner and Ledvina, 2005; Mishin and Burke, 2005; Pfaff et al., 2008, Mishin and Blaunstein, 2008)).

On the basis of experimental observations presented in (Deminov et al, 1995), as well as the theoretical methods summarized in (Blaunstein and Christodoulou, 2007; Blaunstein and Plohotniuc, 2008), the key parameters shown in the table were evaluated and predicted.

Additional peculiarities, which should be mentioned in the conclusions, are as follows:

—Even small irregularities of plasma density $\delta n/n_0 \equiv \sqrt{\langle |\delta N/N_0|^2 \rangle}$ (few percentage points) created during a magnetic storm lead to significant amplitude variations and phase scintillations at frequencies less than 500–600 MHz, while for signals in a band near 1 GHz their intensity is insufficient for the distortion of radio links operating at frequencies of 5–10 GHz.

—Strong fluctuations in plasma density (up to 20%) occurring during strong magnetic storms result in strong and fast fading of radio signals with significant signal intensity oscillations (from 5 to 10%) and phase fluctuations (up to several tens of radians). This effect depends on the frequency of the probing signal and decreases from 1 to 0.1% for the signal intensity and from tens of radians to fractions of a radian for signal phase deviations with increasing frequency.

—In a perturbed ionosphere, the K-parameter changes from a unit to several units which indicates the existence of same-order coherent and incoherent components of signal intensity, that is, indicates the existence of strong multiplicative noises cased by fast fading phenomena, which are fully described by the Ricean law (Blaunstein and Christodoulou, 2007).

Finally, the knowledge of the main parameters of land–satellite communication links passing through a perturbed ionosphere allows for evaluating the main parameters of a signal and channel, such as the capacity and spectral efficiency of the channel, number of errors of digital codes in communication links (BER), etc. These aspects are needed for any additional serious theoretical analysis, and they will be investigated in future.

REFERENCES

Backley, R., Diffraction by Random Phase Screen with Very Large rms Phase Deviation. Two-Dimensional Screen, *Aust. J. Phys.*, 1971, vol. 24, pp. 373–396.

Basu, Su., Basu, Sa., Villadares, C.E., et al., Ionospheric Effects of Major Magnetic Storms during the International Space Weather Period of September and October 1999: GPS Observations, VHF/UHF Scintillations and in situ Density Structures at Middle and Equatorial Latitudes, *J. Geophys. Res.*, 2001, vol. 106, no. 3, pp. 389–399.

Blaunstein, N., Wireless Communication Systems, in *Handbook of Engineering Electromagnetics*, Bansal, R., Ed., New York: Wiley & Sons, 2004, pp. 417–481.

Blaunstein, N. and Christodoulou, Ch., *Radio Propagation and Adaptive Antennas for Wireless Communication Links: Terrestrial, Atmospheric and Ionospheric*, New Jersey: Wiley Intersci., 2007.

Blaunstein, N. and Plohotniuc, E., *Ionosphere and Applied Aspects of Radio Communication and Radar,* New York: CRC Press, Taylor and Frances, 2008.

Booker, H.G., A Theory of Scattering by Non-Isotropic Irregularities with Application to Radar Reflection from the Aurora, *J. Atmos. Terr. Phys.*, 1956, vol. 8, no. 2, pp. 204–221.

Booker, H.G., Application of Refractive Scintillation Theory to Radio Transmission through the Ionosphere and the Solar Wind and to Reflection from a Rough Ocean, *J. Atmos. Terr. Phys.*, 1981, vol. 43, no. 11, pp. 1215–1233.

Booker, H.G. and Gordon, W.E., A Theory of Radio Scattering in the Ionosphere, *Proc. IRE*, 1950, vol. 38, no. 4, pp. 400–412.

Booker, H.G. and Majidi Ahi, G., Theory of Refractive Scattering in Scintillation Phenomena, *J. Atmos. Terr. Phys.*, 1981, vol. 43, no. 11, pp. 1199–1214.

Booker, H.G., Ratcliffe, S.A., and Shinn, D.H., Diffraction from an Irregular Screen with Applications to Ionospheric Problems, *Philos. Trans. R. Soc. London, Ser. A*, 1950, vol. 242, pp. 579–607.

Crain, C.M., Booker, H.G., and Fergusson, S.A., Use of Refractive Scattering to Explain SHF Scintillations, *Radio Sci.*, 1974, vol. 14, no. 1, pp. 125–133.

Deminov, M.G., Karpachev, A.T., Afonin, V.V., Annakuliev, S.K., and Smilauer, J., Dynamics of the Midlatitude Ionospheric Trough during Storms. I. A Qualitative Pattern, *Geomagn. Aeron.*, 1995, vol. 35, no. 1, pp. 73–79.

Denisov, N.G. and Erukhimov, L.M., Statistical Properties of Phase Fluctuations during a Complete Reflection from the Layer, *Geomagn. Aeron.*, 1966, vol. 6, no. 4, pp. 695–702.

Erickson, P., Foster, J., and Holt, J., Inferred Electric Field Variability in the Polarization Jet from Millstone Hill *E* Region Coherent Scatter Radar Observations, *Radio Sci.*, 2002, vol. 37, no. 10, pp. 1027–1036; doi:10.1029/2000RS002531.

Erukhimov, L.M. and Ryzhkov, V.A., Analysis of Focused Ionospheric Irregularities Using Radio-Astronomical Methods at Frequencies of 13–54 MHz, *Geomagn. Aeron.*, 1971, vol. 5, no. 4, pp. 693–697.

Erukhimov, L.M., Komrakov, G.P., and Frolov, V.L., On the Spectrum of Artificial Small-Scale Ionospheric Turbulence, *Geomagn. Aeron.*, 1980, vol. 20, no. 6, pp. 1112–1114.

Farley, D.T., Incoherent Scatter Radar Probing, in *Modern Ionospheric Science*, Kohl, H., Ruster, R., and Schlegel, K., Eds., Katlenburg-Lindau: Copernicus GmbH, 1996, pp. 415–439.

Foster, J. and Burke, W., A New Categorization for Subauroral Electric Fields, *EOS Trans. AGU*, 2002, vol. 83, pp. 393–401.

Foster, J. and Rich, F., Prompt Midlatitude Electric Field Effects during Severe Magnetic Storms, *J. Geophys. Res.*, 1998, vol. 103A, pp. 26 367–26 373.

Gailit, T.A., Gusev, V.D., Erukhimov, L.M., and Shpiro, P.I., On the Spectrum of Phase Fluctuations during Ionospheric Sounding, *Izv. Vyssh. Uchebn. Zaved., Radiofiz.*, 1983, vol. 26, no. 5, pp. 795–801.

Gelberg, M.G., *Neodnorodnosti vysokoshirotnoi ionosfery* (Irregularities of the High-Latitude Ionosphere), Novosibirsk: Nauka, 1986.

Gurevich, A.V., *Nonlinear Phenomena in the Ionosphere*, Berlin: Springer-Verlag, 1978.

Gurevich, A.V. and Tsedilina, E.E., *Sverkhdal'nee rasprostranenie korotkikh radiovoln* (Long-Range Propagation of HF Radiowaves), Moscow: Nauka, 1979.

Guzdar, P., Goncharenko, N., Chaturvedi, P., and Basu, S., Three-Dimensional Nonlinear Simulations of the Gradient Drift Instability in the High-Latitude Ionosphere, *Radio Sci.*, 1998, vol. 33, pp. 1901–1912.

Hardy, D., Schmidt, L., Gussenhoven, M., Marshall, F., Yeh, H., Shumaker, T., Huber, A., and Pantazis, J., *Precipitating Electron and Ion Detectors (SSJ/4) for Block 5D/Flights 4–10 DMSP Satellites: Calibration and Data Presentation*, Massachusetts: Air Force Geophys. Lab., Hansom Air Force Base, 1984.

Hudson, M. and Kelley, M., The Temperature Gradient Instability at the Equatorward Edge of the Ionospheric Plasma Trough, *J. Geophys. Res.*, 1976, vol. 81, no. 22, pp. 3913–3921.

Kadomtsev, B., *Plasma Turbulence*, New York: Acad. Press, 1965.

Keskinen, M., Basu, Su., and Basu, Sa., Mid-Latitude Sub-Auroral Small Scale Structure during a Magnetic Storm, *Geophys. Res. Lett.*, 2004, vol. 31, p. L09811; doi:10.1029/2003GL019368.

Kintner, P. and Ledvina, B.M., The Ionosphere, Radio Navigation, and Global Navigation Satellite Systems, *Adv. Space Res.*, 2005, vol. 35, no. 5, pp. 788–811.

Knepp, D.L., Multiple Phase-Screen Calculation of the Temporal Behavior of Stochastic Waves, *Proc. IEEE*, 1983, vol. 71, pp. 722–737.

Ledvina, B.M., Makela, J.J., and Kitner, P.M., First Observations of Intense GPS L1 Amplitude Scintillations at Midlatitude, *Geophys. Res. Lett.*, 2002, vol. 29, pp. 1659–1662.

Maynard, N., Burke, W., Basinska, E., Erickson, G., Hughes, W., Singer, H., Yahnin, A., Hardy, D., and Mozer, F., Dynamics of the Inner Magnetosphere near Times of Substorm Onsets, *J. Geophys. Res.*, 1996, vol. 101A, pp. 7705–7715.

Mishin, E. and Blaunstein, N., Irregularities within Subauroral Polarization Stream-Related Troughs and GPS Radio Interference at Midlatitudes, *Geophys. Monogr. Am. Geophys. Union*, 2008, no. 181, pp. 291–295; doi:10.1029/181GM26.

Mishin, E.V. and Burke, W.J., Stormtime Coupling of the Ring Current, Plasmasphere and Topside Ionosphere: Electromagnetic and Plasma Disturbances, *J. Geophys. Res.*, 2005, vol. 110A, pp. 7209–7216.

Mishin, E., Burke, W., Huang, C., and Rich, F., Electromagnetic Wave Structures within Subauroral Polarization Streams, *J. Geophys. Res.*, 2003, vol. 108A, pp. 1309–1315.

Pfaff, R., Liebrecht, C., Berthelier, J.-J., Malingre, M., Parrot, M., and Lebreton, J.-P., DEMETER Satellite Observations of Plasma Irregularities in the Topside Ionosphere at Low, Middle, and Sub-Auroral Latitudes and Their Dependence on Magnetic Storms, *Geophys. Monogr. Am. Geophys. Union*, 2008, no. 181, pp. 297–310; doi:10.1029/181GM26.

Rich, F.J. and Hairston, M., Large-Scale Convection Patterns Observed by DMSP, *J. Geophys. Res.*, 1994, vol. 79A, pp. 3827–3835.

Rino, C.L., On the Application of Phase Screen Models to the Interpretation of Ionospheric Scintillation Data, *Radio Sci.*, 1982, vol. 17, pp. 855–867.

Rino, C.L. and Fremouw, E.J., The Angle Dependence of Single Scattered Wave Fields, *J. Atmos. Terr. Phys.*, 1977, vol. 39, no. 8, pp. 859–868.

Saunders, S.R., *Antennas and Propagation for Wireless Communication Systems*, New York: Wiley and Sons, 1999.

Shkarofsky, I.P., Johnston, T.W., and Bachynski, M.P., *The particle Kinetics of Plasmas*, London: Addison-Wesley, 1966.

Titheridge, J.E., The Diffraction of Satellite Signals by Isolated Ionospheric Irregularities, *J. Atmos. Terr. Phys.,* 1971, vol. 33, no. 1, pp. 47–69.

Tsytovich, V.N., *Nonlinear Effects in Plasma*, New York: Plenum Press, 1970.

Wernik, A.W. and Liu, C.H., Application of the Scintillation Theory to Ionospheric Irregularities Studies, *J. Art. Satellites*, 1975, vol. 10, pp. 37–58.